

Chapter 26

Waveform Analysis to Estimate Respiratory Rate

Peter H. Charlton, Mauricio Villarroel and Francisco Salguiero

Learning Objectives

Use the MIMIC II database to compare the performance of multiple algorithms for estimation of respiratory rate (RR) from physiological waveforms.

1. Extract electrocardiogram (ECG), photoplethysmogram (PPG) and thoracic impedance pneumography (IP) waveforms from the MIMIC II database.
2. Identify periods of low quality waveform data.
3. Identify heart beats in the ECG and PPG signals.
4. Estimate RR from the signals.
5. Improve the accuracy of RR estimation using quality assessment and data fusion.
6. Evaluate the performance of RR algorithms.

26.1 Introduction

Respiratory rate (RR) is an important physiological parameter which provides valuable diagnostic and prognostic information. It has been found to be predictive of lower respiratory tract infections [1], indicative of the severity of pneumonia [2], and associated with mortality in paediatric intensive care unit (ICU) patients [3]. Respiratory rate is measured in breaths per minute (bpm). Current routine practice for obtaining RR measurements outside of Critical Care involves manually counting chest movements [4]. This practice is time-consuming, inaccurate [5], and poorly carried out [6–8]. Therefore, there is an urgent need to develop an accurate, automated method for measuring RR in ambulatory patients. Furthermore, an automated method of measuring RR could facilitate: (i) objective patient-led home-monitoring of asthma; (ii) screening for obstructive sleep apnea; and (iii) screening for periods of

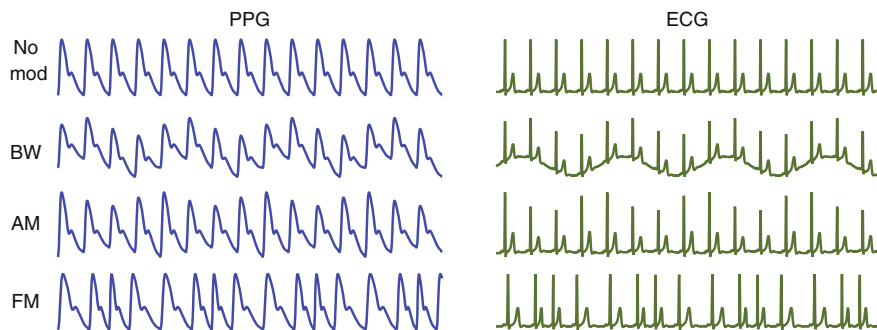


Fig. 26.1 Idealised respiratory modulations of the PPG (*left hand side*) and ECG (*right hand side*). During three respiratory cycles, from *top*: no modulation, baseline wander (BW), amplitude modulation (AM), and frequency modulation (FM). Adapted from [18, 27, 30]

dysregulated breathing during sleep, occasionally seen in advanced congestive heart failure.

A potential solution is to estimate RR from a convenient non-invasive signal which is modulated by respiration and is easily, and preferably routinely, measured. Two such signals are the electrocardiogram (ECG) and the photoplethysmogram (PPG). Both signals exhibit baseline wander (BW), amplitude modulation (AM) and frequency modulation (FM) due to respiration, as shown in Fig. 26.1 (see [9, 10] for further details). Furthermore, both signals can be acquired continuously from ambulatory patients using novel wearable sensors. For example, the SensiumVitals[®] system (Sensium Healthcare) provides continuous ECG monitoring using a lightweight patch with a battery life of up to five days. The ViSi Mobile[®] (Sotera Wireless) provides continuous ECG and PPG monitoring using a wrist-worn monitor with additional ECG electrodes. In addition, non-contact video-based technology is being developed for continuous monitoring of the PPG without the need for any equipment to be attached to a patient [11].

Many algorithms have been developed for estimating RR from the ECG and PPG [10, 12], but have not yet been widely adopted into clinical practice. In this case study we demonstrated the application of exemplary techniques to the ECG and PPG. The performance of these techniques was assessed on an example dataset. The case study is accompanied by MATLAB[®] code, equipping the reader with tools to develop and test their own RR algorithms for estimation of RR from physiological waveforms.

26.2 Study Dataset

PhysioNet's MIMIC II database (Version 3) was chosen for this study since it contains simultaneous ECG, PPG and thoracic impedance pneumography (IP) waveforms [13, 14]. IP signals, usually only measured in critical care, can be

Table 26.1 Criteria for determining whether each of the 100 downloaded MIMIC II database records were included in the analysis

Criterion	Percent of records meeting criterion
Contain all the required waveforms (ECG, PPG and thoracic impedance)	76
Contain all the required numerics [heart rate (HR), pulse rate (PR) and respiratory rate (RR)]	64
Required waveforms and numerics last at least 10 min	51

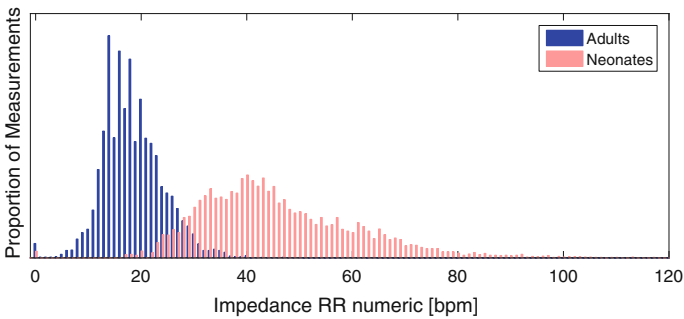


Fig. 26.2 Reference respiratory rate (RR) measurements acquired using thoracic impedance from adults and neonates. The disparity between the distributions of RR measurements acquired from adults (*blue*) and neonates (*red*) prompted a sub-group analysis of these two patient populations

used to estimate reference RRs since individual breaths can be identified as the thoracic impedance increases during inhalation and decreases during exhalation. `MIMICIII_data_importer.m` was used in conjunction with the freely available *WFDB Toolbox*¹ to download the data. One hundred Intensive Care Unit (ICU) stay records, each containing data from a distinct ICU stay, were downloaded.

Records meeting the criteria in Table 26.1 were included in the analysis. The required waveforms and numerics were extracted from the 51 % of records that met these criteria. Each data channel was stored in two vectors of values and corresponding timestamps. This ensured that any gaps in the data due to changes in patient monitoring or data acquisition failures were preserved in the analysis.

Inspection of the dataset revealed a substantial difference in the distributions of IP RR measurements acquired from neonatal and adult patients, as illustrated in Fig. 26.2. This is in keeping with previous findings in [15], in which it was reported that children’s RRs decrease from a median of 43 bpm when younger than

¹*WFDB Toolbox* is available from PhysioNet: <http://physionet.org/physiotools/matlab/wfdb-app-matlab/>.

3 months to a median of 16 bpm when aged 15–18 years. Therefore, we decided to restrict the analysis to adult patients only.

26.3 Pre-processing

The extracted waveforms contained periods of high and low (reliable and unreliable) quality, as shown in Fig. 26.3. This is in keeping with the literature, where it is well reported that physiologic signals can be expected to contain periods of artifact in the Critical Care setting [16]. Each 10 s segment of ECG and PPG data was categorised as either high or low quality using the signal quality indicator (SQI) reported in [17]. This SQI determines the quality of the signal in two steps. Firstly, heart beats are detected to quantify the detected heart rate. Any segments containing physiologically implausible heart rates are deemed to be low quality. Secondly, template matching is used to quantify the correlation between an averaged beat's morphology and that of each individual beat. If the average correlation coefficient across a segment is below an empirical threshold, then the signal quality is deemed to be low (as shown in Fig. 26.4). Low quality segments were eliminated from the analysis.

The RR measurements provided by the clinical monitor were not used as a reference against which to test the accuracy of RR algorithms since they are susceptible to inaccuracies during periods of signal artifact. Instead, reference RRs were extracted from the IP signal, with periods in which reference RRs were unreliable being excluded from the analysis. To do so, the signal was segmented into non-overlapping 32 s windows. Two independent methods were used to estimate RR from each window in line with the methodology presented in [18]. Firstly, Fourier analysis was used to compute the power spectral density of the signal, as described in [19]. A first RR estimate was obtained as the frequency

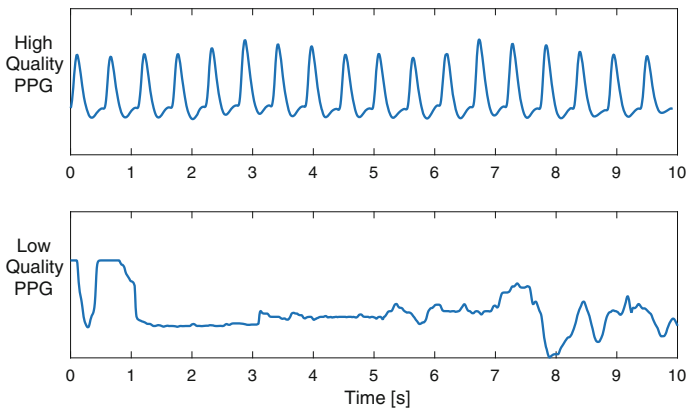


Fig. 26.3 Periods of high and low quality PPG waveform

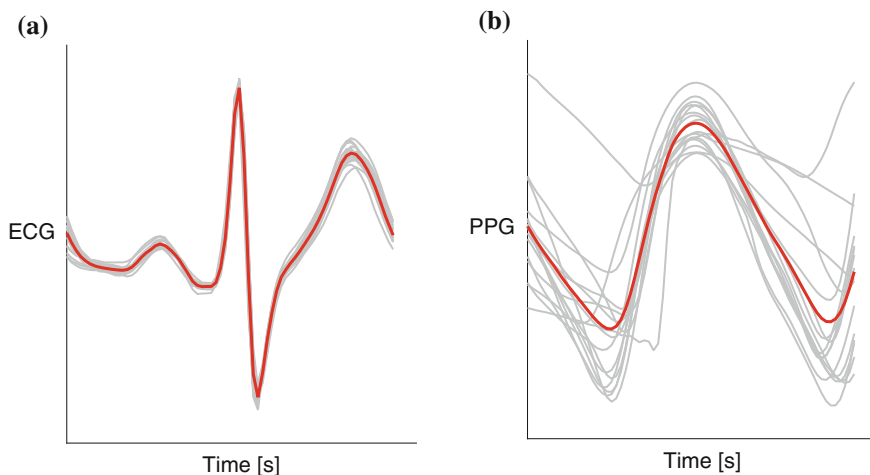


Fig. 26.4 Use of a template-matching signal quality index (SQI) to determine whether a segment of signal is high or low quality. **a** the ECG beats (*grey*) all have a similar morphology to the average beat template (*red*), and the ECG segment is deemed to be high quality. **b** the PPG beats have a highly variable morphology, indicating low signal quality

corresponding to the maximum power within the range of plausible respiratory frequencies (4–60 bpm). Secondly, the “count-orig” method presented in [20] was used to detect individual breaths. A second RR estimate was calculated from the average duration of individual breaths. Count-orig involves normalising the signal, identifying pairs of maxima exceeding a threshold value, and identifying reliable breaths as periods of signal between the pairs of maxima which contain only one minimum below zero. Finally, if the difference between the two RR estimates was < 2 bpm, then the reference RR was calculated as the mean of the two estimates. Otherwise, the window was excluded.

26.4 Methods

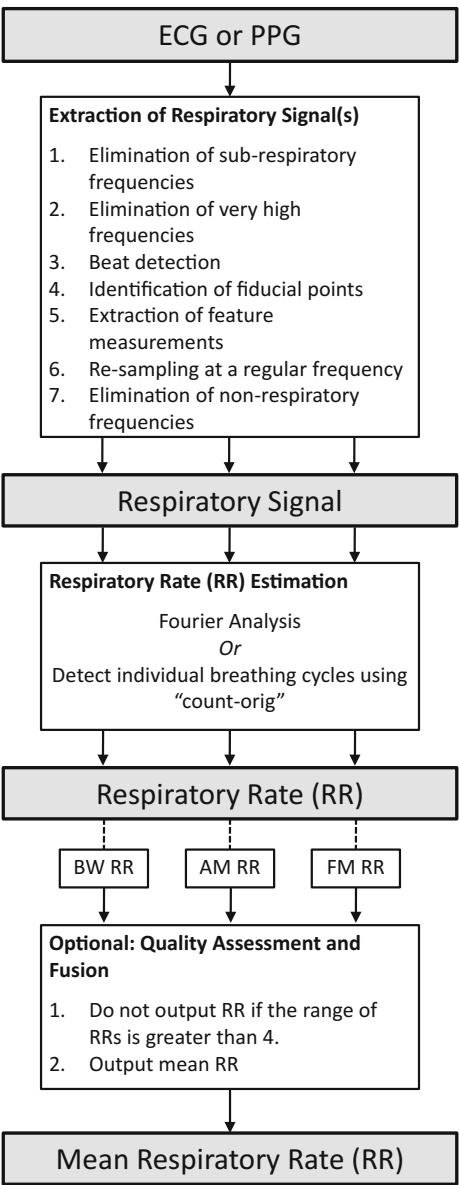
A plethora of algorithms have been proposed for estimation of RR from the ECG or PPG. In this case study we implemented exemplary algorithms (using `RRest.m`) which estimate RR by exploiting one of the three fundamental respiratory modulations, modelled on the approach described in [19]. RR algorithms generally consist of two compulsory components and two optional components. The compulsory components are:

- extraction of a respiratory signal (a time series dominated by respiratory modulation) from the raw signal, and
- estimation of RR from the respiratory signal.

Two optional components, quality assessment and fusion, can be used to improve the accuracy of estimated RRs.

Extraction of a respiratory signal is often performed using a feature-based technique, which extracts a time series of beat-by-beat feature measurements. Figure 26.5 shows the steps involved. The first two steps, the elimination of sub-respiratory (<4 bpm) and very high frequencies (>100 Hz and >35 Hz for the

Fig. 26.5 The steps within a respiratory rate (RR) algorithm. Extraction of respiratory signal(s) and RR estimation are compulsory. The third step consisting of quality assessment and fusion is optional



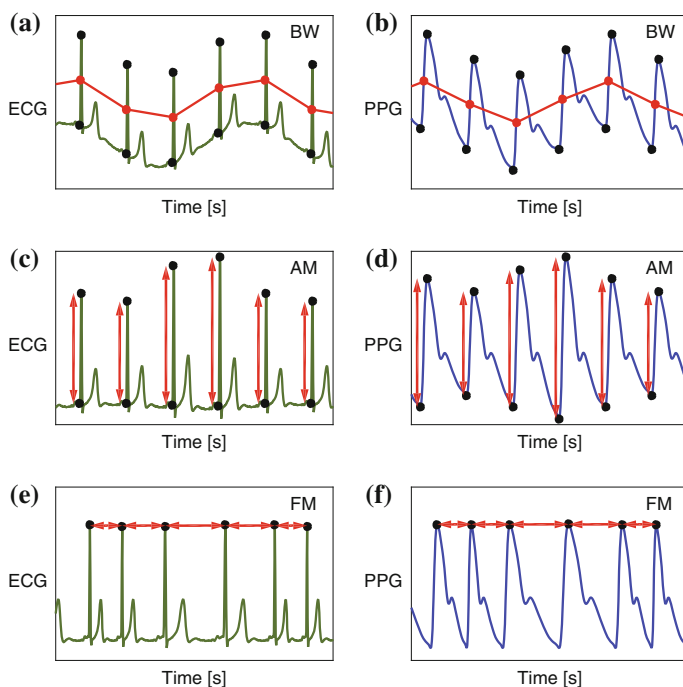


Fig. 26.6 Feature measurement from fiducial points of the ECG and PPG signals. **a** and **b** Measurement of baseline wander (*BW*), the mean of the amplitudes of a beat's peak and trough; **c** and **d** amplitude modulation (*AM*), the difference between the amplitudes of each beat's peak and trough; **e** and **f** frequency modulation (*FM*), the time interval between consecutive peaks

ECG and PPG respectively), are usually not necessary when analysing EHR data since they are often performed by patient monitors prior to signal output. Beat detection was performed in the ECG using a QRS detector based upon the algorithm of Pan, Hamilton and Tompkins [21, 22], and in the PPG using the Incremental-Merge Segmentation (IMS) algorithm [23]. Fiducial points, such as R-waves and pulse-peaks, and Q-waves and pulse troughs, were identified for each beat. Three feature measurements were then extracted from these fiducial points on both the ECG and PPG waveforms as illustrated in Fig. 26.6. The three beat-by-beat time series of feature measurements are sampled irregularly since there is one measurement per heart beat. Since frequency domain analysis requires regularly sampled signals, these signals were resampled at a regular frequency of 5 Hz using linear interpolation. Finally, spurious non-respiratory frequencies introduced in the extraction process were eliminated using band-pass filtering within the range of plausible respiratory frequencies (4–60 bpm). Spurious high frequencies arise due to linear interpolation and spurious low frequencies can be caused by physiological changes.

RR estimation from the ECG and PPG was performed in both the frequency and time domain using the Fourier analysis and breathing cycle detection techniques used to estimate the reference RRs. An additional quality assessment and fusion step, the “Smart Fusion” method [19], was optionally performed in an attempt to increase the accuracy of RR estimates. The first step of “Smart Fusion” is to assess the quality of the RR estimates derived from the three modulations. If the three estimates are within 4 bpm of each other, then a final RR estimate is generated as the mean of the estimates. Otherwise, no output is provided.

26.5 Results

Table 26.2 shows the mean absolute error (MAE) for all methods under analysis. The most accurate algorithm prior to implementing quality assessment and fusion steps had a MAE of 4.28 bpm. This algorithm extracted BW from the PPG and estimated RR using breath detection. Algorithms using BW respiratory signals outperformed those using AM, which in turn outperformed FM algorithms. Furthermore, those using breath detection to estimate RR outperformed those using Fourier analysis.

An improvement in accuracy was observed when the additional quality assessment and fusion step was added to breath detection algorithms. The MAEs for the ECG and PPG decreased from 4.87 to 3.92 bpm, and from 4.28 to 3.36 bpm respectively. This was achieved at the expense of the number of windows from which RRs were estimated. When using this additional step 44 % of ECG windows and 63 % of PPG windows were discarded by the quality assessment. Interestingly, no improvement in accuracy was observed when adding these steps to a Fourier-based algorithm.

It should be noted that a substantial proportion of the data available for analysis was discarded prior to analysis. A reference RR could only be obtained from 10 % of windows. In addition, 44 % of ECG windows, and 30 % of PPG windows were

Table 26.2 The performances of the algorithms applied to the ECG and PPG, measured using the mean absolute error (MAE, measured in breaths per minute, bpm)

Algorithm specification		MAE (bpm)	
Respiratory signal	RR estimation	ECG	PPG
BW	Breath detection	4.87	4.28
AM	Breath detection	4.95	5.58
FM	Breath detection	8.48	7.95
BW	Fourier	7.51	8.18
AM	Fourier	8.69	11.14
FM	Fourier	13.16	12.11
BW, AM, FM	Breath detection + quality assess + fusion	3.92	3.36
BW, AM, FM	Fourier + quality assess + fusion	12.66	10.52

discarded due to low signal quality, likely indicating the presence of movement artifact or sensor disconnection. Consequently, only 6 % of the ECG data, and 7 % of the PPG data were included in the analysis.

26.6 Discussion

RR is widely used in a range of clinical settings to aid diagnosis and prognosis. Despite its clinical importance, it is the only vital sign which is not routinely measured electronically outside of Critical Care. In this case study techniques have been presented for the estimation of RR from two easily and routinely measured physiological signals, the ECG and PPG. There were two important findings. Firstly, the addition of a signal quality and fusion step to the breath-detection algorithms increased accuracy. Secondly, time-domain breath-detection algorithms outperformed the frequency-domain algorithms. This suggests that further research is warranted into time-domain methods, which are far less reliant on the RR being quasi-stationary. If a method is found to perform sufficiently well then it could be used to measure RR during routine physiological assessments to provide early warning of clinical deteriorations.

The dataset used in this case study is a useful resource for further testing of RR algorithms. Its strength is that it contains waveform data from thousands of critically-ill patients, with many datasets lasting hours or days. However, the generalisability of the results is limited by the consisting solely of critically-ill patients. This is particularly significant considering that RR algorithms would most often be used with patients outside of Critical Care. Furthermore, the IP signal gave a reliable reference RR for only 10 % of the time. This resulted in a low number of signal windows being included in the analysis, a significant limitation. Consequently, this case study should be treated as an example of the methodology which could be used to perform a robust study, rather than as a robust study itself. In addition, some uncertainty remained in the reference RRs since they are the mean of two estimates which could differ by up to 2 bpm. When testing algorithms for extraction of clinical parameters from physiological signals, the more accurate the reference value, the better. In this study the measured MAEs are likely to be higher than the true MAEs of the algorithms because of inaccuracies in the reference RR.

A key challenge of waveform analysis is the handling of low quality data. One approach is to detect and exclude low quality data, as performed using the quality assessment and fusion step in this study. A simple template-matching SQI was used here. More complex techniques which fuse the results of multiple SQIs to determine signal quality may improve the performance of RR algorithms in clinical practice [24, 25]. An alternative approach is to refine analysis techniques to ensure they remain accurate even when using low quality data. For instance, in [26] an algorithm is presented for estimation of RR from the ECG during exercise, when the signal is likely to be of low quality.

26.7 Conclusions

This case study demonstrates the potential utility of the ECG and PPG for measurement of RR in the clinical setting. The necessary tools required to design and test RR algorithms are presented, allowing the interested reader to extend this work. The results suggest two particular areas for further algorithmic development. Firstly, the use of signal quality and fusion to improve the accuracy of RR algorithms should be explored further. In the literature much focus has been given to the extraction of respiratory signals and estimation of RR, whereas relatively little research has been conducted into quality assessment and fusion. Secondly, further research should be conducted into the use of time-domain techniques to identify individual breathing cycles. It is notable that in this study the time-domain technique outperformed the frequency-domain technique, whilst in the literature reported time-domain techniques are rarely more sophisticated than peak detection. However, the low data inclusion rate in this study suggests that further investigation is required to ensure that conclusions are robust.

26.8 Further Work

There are two pressing research questions concerning estimation of RR from physiological signals. Firstly, it is not clear which RR algorithm is the most accurate. Until recently validation studies had compared only a few of the many existing algorithms. Comparison between studies is difficult since studies are usually performed on different datasets collected from different populations, using different statistical measures. A recent study evaluated many algorithms on data acquired from young, healthy subjects. Secondly, it is not clear whether the most accurate algorithm performs well enough for clinical use.

Further studies are required to answer such questions. We propose that algorithms should be tested firstly in a healthy population, in ideal operating conditions. This would facilitate assessment of the best possible performance of the algorithms. If any algorithms perform sufficiently well for clinical use, then they could be tested in patient populations in clinical settings. Conversely, if no algorithms perform adequately, then further algorithmic development should be carried out to attempt to improve the performance. The MIMIC II database provides opportunity to test algorithms in a wide range of physiological conditions, such as hyper- and hypotension, and normal and reduced ejection fraction. This may provide insight into the limitations of the algorithms, ensuring that they are only used when in conditions in which they can be expected to perform well.

26.9 Non-contact Vital Sign Estimation

As presented in this chapter, current monitoring systems available to track changes in the vital signs of patients in the clinic or at home require contact with the subject. Most patients requiring regular monitoring find the probes difficult to attach and use properly [28]. The process of recording vital signs, even if it only takes a few minutes, becomes burdensome as it usually has to be performed on a daily basis. The low compliance of patients with wearing sensors is also an obstacle to successful monitoring.

The ideal technology to estimate vital signs would involve sensors with no direct contact with the patient, providing several advantages over traditional methods because no subject participation is required to set the equipment up, it requires no skin preparation, causes no skin irritation, decreases the risk of infection, and has the potential to be seamlessly integrated into the patient's lifestyle.

Several technologies have been proposed for non-contact monitoring of vital signs from Radar-based systems to non-contact ECG using capacitive coupling electrodes. During the last decade, with the cost of digital video cameras continuing to decrease as the technology becomes more ubiquitous, research in non-contact vital sign monitoring has expanded through the use of off-the-shelf video cameras. Video cameras can be found in laptops, mobile phones, set-top boxes and television sets in patients' living room, opening up new possibilities for the monitoring of vital signs.

Video-based vital sign monitoring extends the concepts of traditional photoplethysmography using the multiple photosites present in an imaging sensor to record the blood volume changes associated with the cardiac cycle. These physiological changes result in a waveform known as photoplethysmographic imaging (PPGi), from which vital signals such as heart rate, respiratory rate, oxygen saturation (SpO_2) and other can be estimated [11, 29]. Figure 26.7 shows a 15-s sample of PPGi alongside PPG and IP signals measured using conventional monitoring equipment. The patient was undergoing haemodialysis treatment at the Churchill Hospital in Oxford. During this period the patient had a heart rate of 60 beats/min and a respiratory rate of 15 bpm, both of which can be computed from both the conventional monitoring equipment and the camera using the methods explained in this chapter.

Decades of extensive research from the computer vision community have helped to develop imaging systems that are capable of complex computations (such as face detection, identity access control or other object tracking), are interactive (such as motion/gesture and body tracking in games) and can perform complex 3D reconstruction operations. Therefore, video-based vital sign monitoring has the potential to expand the role vital sign monitoring beyond that which can be met by traditional pulse oximetry.

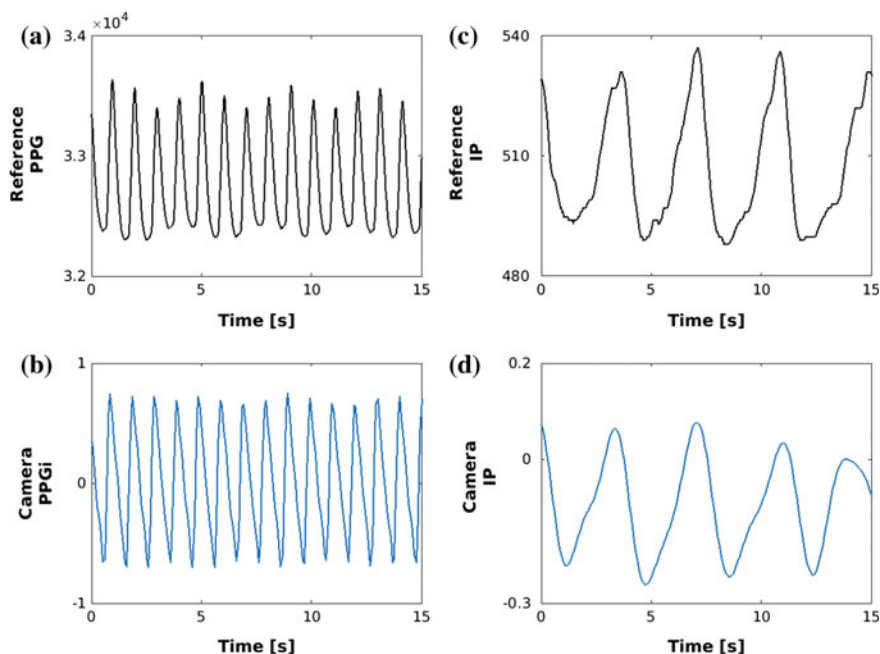


Fig. 26.7 A 15-s sample of data from a patient undergoing haemodialysis treatment at the Churchill Hospital in Oxford. **a** Reference PPG waveform from a Nonin pulse oximeter, **b** extracted photoplethysmographic imaging (PPGi) waveform from a video camera, **c** reference impedance pneumography (IP) respiratory signal, **d** respiratory signal extracted from the PPGi waveform. During the period the patient had a heart rate of 60 beats/min and a respiratory rate of 15 breaths per minute (bpm)

Open Access This chapter is distributed under the terms of the Creative Commons Attribution-NonCommercial 4.0 International License (<http://creativecommons.org/licenses/by-nc/4.0/>), which permits any noncommercial use, duplication, adaptation, distribution and reproduction in any medium or format, as long as you give appropriate credit to the original author(s) and the source, a link is provided to the Creative Commons license and any changes made are indicated.

The images or other third party material in this chapter are included in the work's Creative Commons license, unless indicated otherwise in the credit line; if such material is not included in the work's Creative Commons license and the respective action is not permitted by statutory regulation, users will need to obtain permission from the license holder to duplicate, adapt or reproduce the material.

Code Appendix

The code used in this case study is available from the GitHub repository accompanying this book: <https://github.com/MIT-LCP/critical-data-book>. Further information on the code is available from this website. The following key scripts were used:

- `MIMICII_data_importer.m`: used to extract data from the MIMIC II database.
- `RRest.m`: used to run RR algorithms and assess their performances.

References

1. Shann F, Hart K, Thomas D (1984) Acute lower respiratory tract infections in children: possible criteria for selection of patients for antibiotic therapy and hospital admission. *Bull World Health Organ* 62(5):749
2. Lim WS, Van der Eerden MM, Laing R, Boersma WG, Karalus N, Town GI, Lewis SA, Macfarlane JT (2003) Defining community acquired pneumonia severity on presentation to hospital: an international derivation and validation study. *Thorax* 58(5):377–382
3. Pollack MM, Ruttimann UE, Getson PR (1988) Pediatric risk of mortality (prism) score. *Crit Care Med* 16(11):1110–1116
4. World Health Organization (WHO) (1990) Fourth Programme Report, 1988–1989: ARI Programme for Control of Acute Respiratory Infections. Technical Report, WHO, Geneva
5. Lovett PB, Buchwald JM, Stürmann K, Bijur P (2005) The vexatious vital: neither clinical measurements by nurses nor an electronic monitor provides accurate measurements of respiratory rate in triage. *Ann Emerg Med* 45(1):68–76
6. Chellel A, Fraser J, Fender V, Higgs D, Buras-Rees S, Hook L, Mummery L, Cook C, Parsons S, Thomas C (2002) Nursing observations on ward patients at risk of critical illness. *Nurs Times* 98(46):36–39
7. Cretikos MA, Bellomo R, Hillman K, Chen J, Finfer S, Flabouris A (2008) Respiratory rate: the neglected vital sign. *Med J Aust* 188(16):657–659
8. Hogan J (2006) Why don't nurses monitor the respiratory rates of patients? *Br J Nurs* 15(9):489–492
9. Meredith DJ, Clifton D, Charlton P, Brooks J, Pugh CW, Tarassenko L (2012) Photoplethysmographic derivation of respiratory rate: a review of relevant physiology. *J Med Eng Technol* 36(1):1–7
10. Bailon R, Sornmo L, Laguna P (2006) ECG-derived respiratory frequency estimation. In: *Advanced methods and tools for ECG data analysis* (Chap. 8). Artech House, London, pp 215–244
11. Tarassenko L, Villarroel M, Guazzi A, Jorge J, Clifton DA, Pugh C (2014) Non-contact video-based vital sign monitoring using ambient light and auto-regressive models. *Physiol Meas* 35(5):807–831
12. Garde A, Karlen W, Ansermino JM, Dumont GA (2014) Estimating respiratory and heart rates from the correntropy spectral density of the photoplethysmogram. *PLoS ONE* 9(1): e86427
13. Goldberger AL, Amaral LA, Glass L, Hausdorff JM, Ivanov PC, Mark RG, Mietus JE, Moody GB, Peng CK, Stanley HE (2000) Physiobank, physiotoolkit, and physionet components of a new research resource for complex physiologic signals. *Circulation* 101(23): E215–E220
14. Saeed M, Villarroel M, Reisner AT, Clifford G, Lehman L, Moody G, Heldt T, Kyaw TH, Moody B, Mark RG (2011) Multiparameter intelligent monitoring in intensive care II: a public-access intensive care unit database. *Crit Care Med* 39(5):952–960
15. Fleming S, Thompson M, Stevens R, Heneghan C, Plüddemann A, Maconochie I, Tarassenko L, Mant D (2011) Normal ranges of heart rate and respiratory rate in children from birth to 18 years of age: a systematic review of observational studies. *Lancet* 377(9770):1011–1018

16. Nizami S, Green JR, McGregor C (2013) Implementation of artifact detection in critical care: a methodological review. *IEEE Rev Biomed Eng* 6:127–142
17. Orphanidou C, Bonnici T, Charlton P, Clifton D, Vallance D, Tarassenko L (2015) Signal-quality indices for the electrocardiogram and photoplethysmogram: derivation and applications to wireless monitoring. *IEEE J Biomed Health Inform* 19(3):832–838
18. Pimentel MAF, Charlton PH, Clifton DA (2015) Probabilistic estimation of respiratory rate from wearable sensors. In: Mukhopadhyay SC (ed) *Wearable electronics sensors*, vol 15. Springer International Publishing, pp 241–262
19. Karlen W, Raman S, Ansermino JM, Dumont GA (2013) Multiparameter respiratory rate estimation from the photoplethysmogram. *IEEE Trans Biomed Eng* 60(7):1946–1953
20. Schäfer A, Kratky KW (2008) Estimation of breathing rate from respiratory sinus arrhythmia: comparison of various methods. *Ann Biomed Eng* 36(3):476–485
21. Pan J, Tompkins WJ (1985) A real-time QRS detection algorithm. *IEEE Trans Biomed Eng* 32(3):230–236
22. Hamilton PS, Tompkins WJ (1986) Quantitative investigation of QRS detection rules using the MIT/BIH arrhythmia database. *IEEE Trans Biomed Eng* 33(12):1157–1165
23. Karlen W, Ansermino JM, Dumont G (2012) Adaptive pulse segmentation and artifact detection in photoplethysmography for mobile applications. In: *Proceedings of the annual international conference of the IEEE engineering in medicine and biology society*, vol 2012. EMBS, pp 3131–3134
24. Behar J, Oster J, Li Q, Clifford GD (2013) ECG signal quality during arrhythmia and its application to false alarm reduction. *IEEE Trans Biomed Eng* 60(6):1660–1666
25. Li Q, Clifford GD (2012) Dynamic time warping and machine learning for signal quality assessment of pulsatile signals. *Physiol Meas* 33(9):1491–1501
26. Bailón R, Sömmo L, Laguna P (2006) A robust method for ECG-based estimation of the respiratory frequency during stress testing. *IEEE Trans Biomed Eng* 53(7):1273–1285
27. Charlton PH, Bonnici T, Tarassenko L, Clifton DA, Beale R, Watkinson PJ (2016) An assessment of algorithms to estimate respiratory rate from the electrocardiogram and photoplethysmogram. *Physiol Measur* 37(4): 610–626
28. Bonnici T, Orphanidou C, Vallance D, Darrell A, Tarassenko L (2012) Testing of wearable monitors in a real-world hospital environment: what lessons can be learnt? In: *2012 ninth international conference on wearable and implantable body sensor networks*, pp 79–84
29. Villarroel M, Guazzi A, Jorge J, Davis S, Watkinson P, Green G, Shenvi A, McCormick K, Tarassenko L (2014) Continuous non-contact vital sign monitoring in neonatal intensive care unit. *Healthc Technol Lett* 1(3):87–91
30. Addison PS, Watson JN, Mestek ML, Mecca RS (2012) Developing an algorithm for pulse oximetry derived respiratory rate (RR(oxi)): a healthy volunteer study. *J Clin Monit Comput* 26(1):45–51